Journal of Pharmaceutical and Biomedical Analysis 51 (2010) 768–773

Contents lists available at ScienceDirect

Journal of Pharmaceutical and Biomedical Analysis

journal homepage: www.elsevier.com/locate/jpba

Short communication

Interaction of kaempferol with human serum albumin: A fluorescence and circular dichroism study

Iulia Matei, Mihaela Hillebrand*

Department of Physical Chemistry, Faculty of Chemistry, University of Bucharest, Bd. Regina Elisabeta, No. 4–12, Bucharest, Romania

ARTICLE INFO

Article history:
Received 7 July 2009
Received in revised form
22 September 2009
Accepted 24 September 2009
Available online 1 October 2009

Keywords:
Flavonoid
Serum albumin
Fluorescence
Circular dichroism
Thermodynamic parameters
Förster resonance energy transfer

ABSTRACT

The interaction of kaempferol (kaemp), a natural flavonoid to which antioxidative, anti-inflammatory and cardio-protective biological activities have been attributed, with human serum albumin (HSA), the main *in vivo* transporter of exogenous substances, was investigated by steady-state, synchronous fluorescence and circular dichroism spectroscopies. The binding constant, K, and number of binding sites, n, were computed using literature models that showed satisfactory agreement and revealed a strong interaction ($K \sim 3.5 \times 10^5\ M^{-1}$, $n \sim 1$). The binding process was investigated at temperatures in the range 298–313 K, allowing for the evaluation of the thermodynamic parameters, which indicate the occurrence of hydrogen bonding interactions. The distance between kaemp and the tryptophan residue of HSA was estimated at 2.7 nm using Förster's theory of nonradiative resonance energy transfer. Using circular dichroism we evidenced some degree of HSA defolding upon binding.

1. Introduction

Kaempferol (kaemp) (Scheme 1) belongs to the flavonoid class, a large group of polyphenolic compounds widely distributed in higher plants. Due to their abundance in the human diet, their bioavailability and biological properties have raised a great interest in the last two decades [1]. Dietary flavonoids are receiving increasing attention as potential protectors against a variety of diseases, due to their antioxidant, anti-inflammatory, anticoagulant and cardiovascular-protective activities [2–4]. A deep understanding of the way flavonoids are absorbed, metabolized, transported and delivered to the specific tissues is required in order to demonstrate the relationship between a flavonoid-rich diet and health. The mechanisms of these processes are only partially understood, the complex microenvironments of the binding sites of flavonoids with proteins being scarcely explored.

Human serum albumin (HSA), the most abundant protein in blood plasma, plays a major role in the transport and deposition of endogenous and exogenous ligands. Since the affinity towards HSA influences the overall distribution, metabolism and efficacy of the ligands, the investigation of their binding to HSA is of fundamental significance. HSA is a globular protein consisting of a single polypeptide chain with 585 amino acids, but only one tryptophan residue (Trp214) [5]. The main binding sites of aromatic and heterocyclic ligands on HSA are within two hydrophobic pockets in subdomains IIA and IIIA, namely Sudlow sites I and II [6]. Sudlow site I is of major importance, as it contains the Trp214 residue.

By using spectroscopic methods, the high affinity of flavonoids towards serum albumins has recently been reported [7–10]. Kanakis et al. [11] investigated the kaemp–HSA interaction by means of absorption and FTIR spectroscopies, at room temperature. In order to get a complete view on the binding process, in the present study we examined this interaction at various temperatures by using the more sensitive method of steady-state fluorescence spectroscopy combined with other methods that offer information on the effects of complexation on the protein secondary structure, *i.e.* circular dichroism and synchronous fluorescence. We determined the characteristics of the binding, *i.e.* binding constant, number and type of binding sites, nature of binding forces, as well as the effects of complexation on the protein secondary structure. In addition to the previous study, we computed the thermodynamic and Förster parameters associated with the binding process.

2. Materials and methods

The absorption and circular dichroism spectra were recorded on a V-560 Jasco UV-VIS spectrophotometer and on a Jasco J-815 CD spectrometer, respectively. The fluorescence spectra were

* Corresponding author. Tel.: +40 213143508; fax: +40 213159249.
E-mail address: mihh@gw-chimie.math.unibuc.ro (M. Hillebrand).

0731-7085/$ – see front matter © 2009 Published by Elsevier B.V.
doi:10.1016/j.jpba.2009.09.037

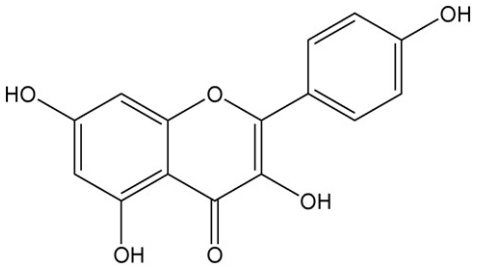

Scheme 1. Molecular structure of kaempferol.

recorded on a FP-6300 Jasco spectrofluorimeter equipped with a STR-313 Jasco thermostatic cell holder. Human serum albumin was purchased from Fluka (fatty acids free, 99%) and kaempferol was obtained from Sigma and used without further purification.

HSA solutions 3×10^{-6} M (for fluorescence) and 0.75×10^{-6} M (for circular dichroism) were prepared in phosphate buffer (pH 7.4; 0.1M) and equilibrated over night. A stock solution of kaemp in methanol (3.3×10^{-4} M) was diluted with phosphate buffer to yield a 3.3×10^{-5} M solution used in titration experiments. This low amount of methanol does not affect the structure of HSA [11]. Binding of kaemp to HSA was studied by the fluorescence quenching titration method using the intrinsic fluorescence of HSA as a probe, at constant HSA concentration and various kaemp concentrations to obtain complexes in the range of drug to protein (d/p) molar ratio 0–4. The steady-state fluorescence spectra were obtained using an excitation wavelength of 286 nm (excitation of the Trp and tyrosine, Tyr, residues) and the emission was measured at 343 nm. Experiments using λ_{ex} = 295 nm (excitation of Trp) did not lead to different results. Synchronous fluorescence spectra were obtained using $\Delta\lambda$ = 15 nm (Tyr excitation) and 60 nm (Trp excitation), where $\Delta\lambda = \lambda_{em} - \lambda_{ex}$. The titration was performed at five temperatures (298, 300, 303, 308 and 313 K). The circular dichroism spectra of free HSA and kaemp–HSA complexes were scanned in the range 200–280 nm, in order to record the characteristic signal of the α-helix conformation of the albumin.

3. Results and discussion

3.1. Quenching of HSA fluorescence by kaempferol

Upon excitation at 286 nm, strong emission from HSA (λ_{em} = 343 nm) and no emission from kaemp were registered in the emission range 300–500 nm. The fluorescence of HSA was quenched upon interaction with kaemp, in a concentration-dependent manner (Fig.1), for all temperatures.

Quenching can appear as result of various inter and intramolecular interactions, *i.e.* molecular collisions (dynamic quenching), complex formation (static quenching), energy transfer and/or conformational changes [12]. Therefore, quenching of the intrinsic HSA fluorescence by kaemp offers information on the binding process. Fluorescence quenching is described by the Stern–Volmer (SV) equation [13]:

$$\frac{F_0}{F} = 1 + K_{SV}[Q] \quad (1)$$

where F_0 and F are the steady-state fluorescence intensities in the absence and presence of kaemp, respectively, K_{SV} is the Stern–Volmer quenching constant and [Q] is the quencher concentration. Function of temperature, one can observe three trends of the SV plots (inset A of Fig. 1): positive deviation at 298 and 300 K, typical linear plot at 303 K and negative deviation at 308 and 313 K. The shape of the SV plot gives indications on the quenching mechanism involved: a linear plot suggests the predominance of dynamic quenching, an upward curvature indicates an additional,

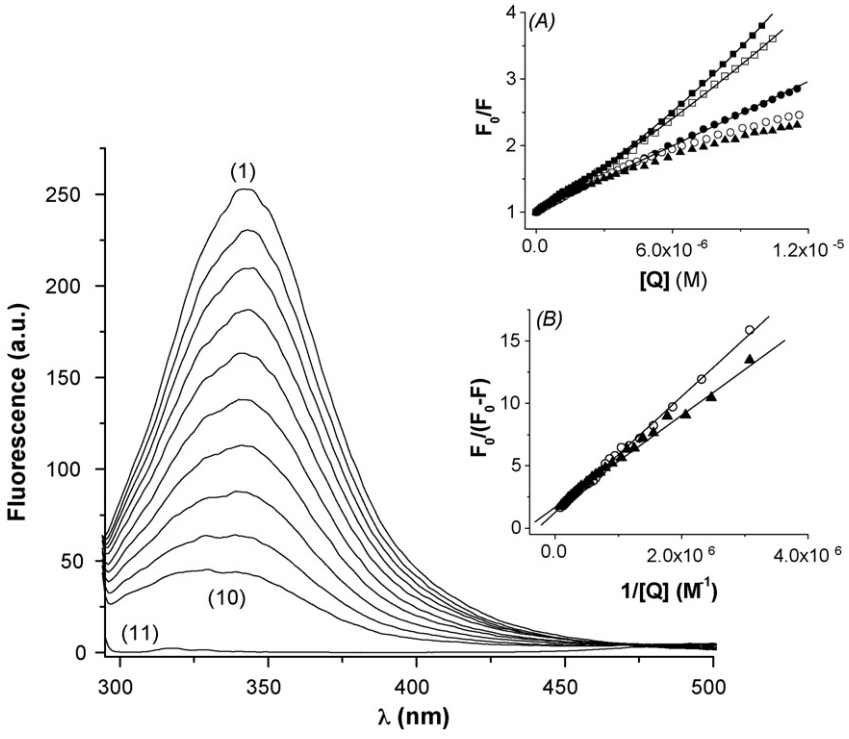

Fig. 1. Fluorescence spectra of HSA (3×10^{-6} M) in the presence of increasing amounts of kaemp; d/p corresponds to 0, 0.11, 0.24, 0.42, 0.67, 0.99, 1.43, 1.93, 2.62 and 3.50 from (1) to (10); (11) is kaemp alone (3.3×10^{-5} M); pH = 7.4, T = 298 K, λ_{ex} = 286 nm, λ_{em} = 343 nm. Inset (A): Stern–Volmer plots for the quenching of HSA by kaemp in the d/p range 0–4, at 298 K (■), 300 K (□), 303 K (●), 308 K (○) and 313 K (▲). The continuous lines represent fits for the linear dependence (Eq. (1)) and positive deviations (Eq. (2)). Inset (B): fits for the negative deviations (Eq. (3)).

Table 1
Parameters characterizing the quenching of HSA by kaemp.

T (K)	SV plot	K_{SV} ($\times 10^{-5}$ M^{-1})	f	V (M^{-1}); r_q (nm)	d/p range	R^a; SD^b; N^c
298	2 linear	2.22 ± 0.01	–	–	0–1.0	0.999; 0.009; 31
		3.15 ± 0.02			1.0–3.5	0.999; 0.017; 14
	Positive	1.81 ± 0.04	–	30680; 22	0–3.5	0.999; 0.023; 45
300	2 linear	2.13 ± 0.02	–	–	0–1.5	0.998; 0.013; 29
		2.70 ± 0.01			1.5–3.5	0.999; 0.009; 14
	Positive	1.98 ± 0.04	–	15584; 18	0–3.5	0.999; 0.022; 43
303	Linear	1.61 ± 0.01	–	–	0–4.0	0.999; 0.017; 46
308	Negative	2.49 ± 0.01	0.84	–	0–4.0	0.999; 0.167; 43
313	Negative	4.54 ± 0.01	0.60	–	0–4.0	0.996; 0.293; 43

[a] R is the correlation coefficient.
[b] SD is the standard deviation of the fit.
[c] N is the number of experimental points considered for the fit.

static component [12] while a downward curvature appears when a fluorophore fraction is not accessible to the quencher [14].

For the linear SV dependency, Eq. (1) was applied to determine K_{SV}. The positive deviation cases were analysed either considering two linear dependencies (d/p domains 0–1 and 1–4) or by using a modified SV equation accounting for simultaneous static and dynamic mechanisms [13]:

$$\frac{F_0}{F} = (1 + K_{SV}[Q])\exp(V \times [Q]) \quad (2)$$

where V is the volume of the quenching sphere, which allows estimation of the quenching distance, r_q. For negative deviation cases the following equation was used [15]:

$$\frac{F_0}{F_0 - F} = \frac{1}{f} + \frac{1}{fK[Q]} \quad (3)$$

where f is the fluorophore fraction available to the quencher. The fits and corresponding regression data are given in Fig. 1 (insets A and B) and Table 1, respectively. The value of the quenching rate constant k_q was also computed, according to $k_q = K_{SV}/\tau_0$, where τ_0 is the excited state lifetime of the fluorophore [12]. Taking $K_{SV} \sim 10^5$ M^{-1} and τ_0 of HSA $\sim 10^{-8}$ s [16], a value of $k_q \sim 10^{13}$ M^{-1} s^{-1} was obtained, which exceeds the maximum rate constant for diffusional quenching in biopolymers of 2×10^{10} M^{-1} s^{-1} [17]. This supports our assertion that complex formation plays a significant role in this quenching process.

3.2. Binding parameters

The estimation of the association constant, K, and number of binding sites, n, of the kaemp–HSA system was done using three models that take into account the presence of a single class of n independent binding sites. The first model, Eq. (4), starts from

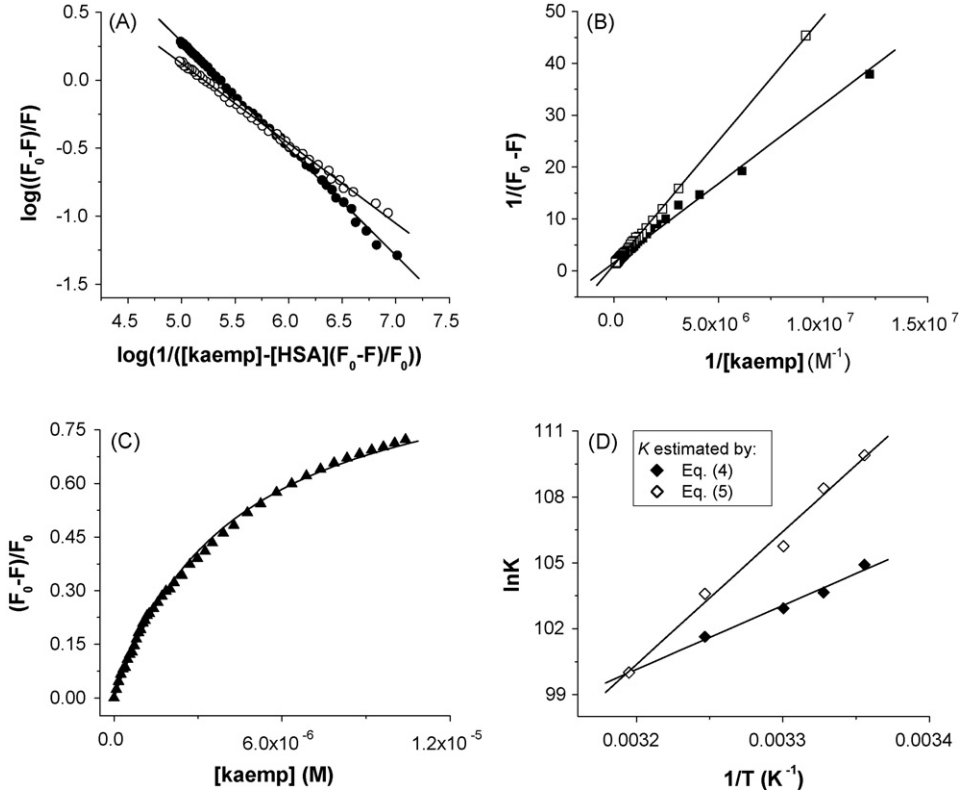

Fig. 2. (A–C) Plots for the determination of the binding parameters according to Eqs. (4)–(6), at 298 K (■), 300 K (▲), 303 K (●), 308 K (□) and 313 K (○). [HSA] = 3×10^{-6} M, d/p = 0–4, λ_{ex} = 286 nm, λ_{em} = 343 nm. (D) Van't Hoff plots according to Eq. (7).

Table 2
Binding parameters characterizing the kaemp–HSA interaction.

Model	T (K)	K ($\times 10^{-5}$ M^{-1})	n	d/p range	R^a; SD^b; N^c
Eq. (4)	298	2.89 ± 0.12	0.65	0–1.6	0.995; 0.033; 27
		3.31 ± 0.03	1.11	1.6–3.5	0.999; 0.006; 13
	300	2.49 ± 0.17	0.61	0–0.7	0.996; 0.033; 19
		3.46 ± 0.02	0.90	0.7–3.5	0.999; 0.012; 22
	303	2.29 ± 0.02	0.79	0–4.0	0.999; 0.027; 47
	308	1.97 ± 0.01	0.61	0.7–4.0	0.999; 0.007; 26
	313	1.62 ± 0.03	0.59	0–4.0	0.999; 0.020; 43
Eq. (5)	298	5.31 ± 0.38	–	0–3.5	0.996; 0.582; 43
	300	4.43 ± 0.24	–	0–3.5	0.998; 0.403; 41
	303	3.23 ± 0.37	–	0–4.0	0.995; 0.949; 45
	308	2.49 ± 0.06	–	0–4.0	0.999; 0.167; 45
	313	4.54 ± 0.20	–	0–4.0	0.996; 0.293; 43
Eq. (6)	298	3.56 ± 0.10	1.02	1.0–3.5	0.999; 0.007; 19
	300	2.94 ± 0.01	0.71	1.0–3.5	0.999; 0.002; 18

[a] R is the correlation coefficient.
[b] SD is the standard deviation of the fit.
[c] N is the number of experimental points considered for the fit.

the classical Scatchard equation [18] and expresses the free ligand concentration at equilibrium as function of the total ligand concentration [8]:

$$\log\frac{F_0-F}{F} = n\log\frac{1}{[\text{kaemp}]-[\text{HSA}]\frac{F_0-F}{F_0}} + n\log K \quad (4)$$

where [kaemp] and [HSA] are total concentrations. Linear fits according to Eq. (4) for two temperatures are shown as an example in Fig. 2. Results indicate a strong interaction between kaemp and HSA, with $K \sim 3\times10^5$ M^{-1} at 298 K (Table 2). The n value approaches unity, suggesting that one molecule of kaemp combines with one molecule of HSA.

Use of the Lineweaver–Burk model, which is based on an equation similar to the modified SV equation for negative deviations [19] (Eq. (5)), predicts slightly higher K values. Here K is in fact the quenching constant describing the binding efficiency of the quencher to the fluorophore [17]:

$$\frac{1}{F_0-F} = \frac{1}{F_0} + \frac{1}{KF_0[\text{kaemp}]} \quad (5)$$

The nonlinear regression model proposed by Guo et al. [20] (Eq. (6)) only gave satisfactory results for the linear and positive quenching cases, when considering the points at $d/p > 1$:

$$\frac{F_0-F}{F_0} = \frac{1}{2}\left(1+\frac{1}{nK[\text{HSA}]}+\frac{[\text{kaemp}]}{n[\text{HSA}]}\right) - \frac{1}{2}\sqrt{\left(1+\frac{1}{nK[\text{HSA}]}+\frac{[\text{kaemp}]}{n[\text{HSA}]}\right)^2 - \frac{4[\text{kaemp}]}{n[\text{HSA}]}} \quad (6)$$

In conclusion, we can state that these models are consistent in a satisfactory manner, indicating a strong interaction between kaemp and HSA, with 1:1 stoichiometry and $K \sim 3.5\times10^5$ M^{-1} at 298 K. This is in good accordance with the value 2.6×10^5 M^{-1} obtained by Kanakis et al. [11] by UV–vis spectroscopy.

3.3. Thermodynamic parameters and the nature of the binding forces

The enthalpy (ΔH), entropy (ΔS) and free energy (ΔG) changes characterizing the binding process are the main evidence in determining the forces (hydrophobic, hydrogen bonding, van der Waals, electrostatic) acting between kaemp and HSA. Under the premise of constant ΔH when the temperature variation is not large, the thermodynamic parameters characterizing the binding were calculated using the Van't Hoff equation [21] (Fig. 2D):

$$\ln K = -\frac{\Delta H}{RT} + \frac{\Delta S}{R} \quad (7)$$

where T is the absolute temperature and R is the gas constant. ΔG was then estimated according to $\Delta G = \Delta H - T\Delta S$. When using K values obtained by Eq. (4), the thermodynamic parameters were $\Delta H = -29.82$ kJ/mol, $\Delta S = 0.004$ kJ/(mol K) and $\Delta G = -31.13$ kJ/mol and when Eq. (5) K values were used, the parameters were -59.15 kJ/mol, -0.089 kJ/(mol K) and -32.63 kJ/mol, respectively. Both models indicate that the binding process is enthalpy-driven and the large negative ΔH together with the very small ΔS suggest the presence of hydrogen bonding interactions [22].

3.4. Effect of kaemp on the conformation of HSA

3.4.1. Synchronous fluorescence measurements. The nature of the binding site

Information on the molecular environment in the vicinity of the Trp and Tyr fluorophores of HSA was obtained by synchronous fluorescence, which offers the advantages of spectral simplification and bandwidth reduction [23]. Thus, we obtained the characteristic spectra of the Trp and Tyr residues, using $\Delta\lambda = 60$ nm and 15 nm, respectively (not shown). No significant shifts in the position of the synchronous maxima were registered, but a stronger fluorescence quenching was noticed for Trp ($F_{(d/p=0)}/F_{(d/p=4)} = 5.8$) compared to that of Tyr ($F_{(d/p=0)}/F_{(d/p=4)} = 2.7$), indicating that the binding site of kaemp is nearer to the Trp residue. Therefore, it can be inferred that the primary binding site of kaemp is the Sudlow site I of HSA, in accordance with the previously reported localization of flavonoids [7,24].

3.4.2. Circular dichroism measurements

It is known that ligand binding to a globular protein can alter the secondary structure, resulting in changes in the protein conformation, which are reflected by the circular dichroism (CD) spectrum. The CD spectrum of HSA exhibits two negative bands at 209 and 222 nm, characteristic for the α-helix structure [25]. Fig. 3 shows the changes in HSA α-helicity upon kaemp addition.

The helical content of free and bound HSA was calculated from the mean residue ellipticity (MRE, Eq. (8)) values at 209 nm, using Eq. (9) [26]:

$$\text{MRE} = \frac{\theta}{10rl[\text{HSA}]}\ (\text{in units of } deg\ \text{cm}^2\ \text{dmol}^{-1}) \quad (8)$$

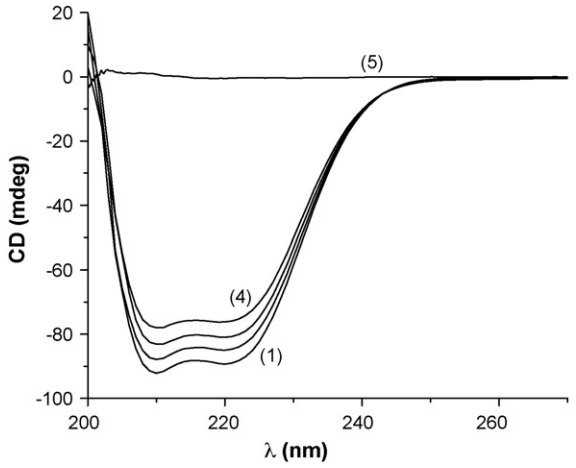

Fig. 3. The CD spectra of HSA 0.75×10^{-6} M (1), kaemp–HSA system at $d/p = 1$ (2), 3 (3) and 6 (4), and kaemp 3.3×10^{-6} M (5). pH = 7.4, $T = 298$ K.

θ is the observed CD (in milli-degrees), $r = 585$ (number of HSA amino acid residues) and l is the path length of the cell (in cm):

$$\%\,\alpha\text{-helix} = \frac{-\mathrm{MRE}_{209\,\mathrm{nm}} - 4000}{33000 - 4000} \times 100 \quad (9)$$

The α-helix percent decreases gradually, from 58.1% in free HSA to 55.8% upon kaemp binding at $d/p = 6$, indicating some degree of HSA defolding.

3.4.3. Energy transfer efficiency and binding distance

The distance r between the Trp of HSA and the kaemp molecule was determined by Förster resonance energy transfer (FRET) [27], the distance dependent interaction in which excitation energy is transferred nonradiatively from HSA (donor, D) to kaemp (acceptor, A), as long as an overlap exists between the emission spectrum of D and the absorption spectrum of A (Fig. 4).

The following well-known equations were used:

$$E = \frac{R_0^6}{R_0^6 + r^6} = 1 - \frac{F}{F_0} \quad (10)$$

$$R_0^6 = 8.8 \times 10^{-25} k^2 n^{-4} \Phi J \quad (11)$$

$$J = \int_0^\infty F_\mathrm{D}(\lambda)\varepsilon_\mathrm{A}(\lambda)\lambda^4\, d\lambda \quad (12)$$

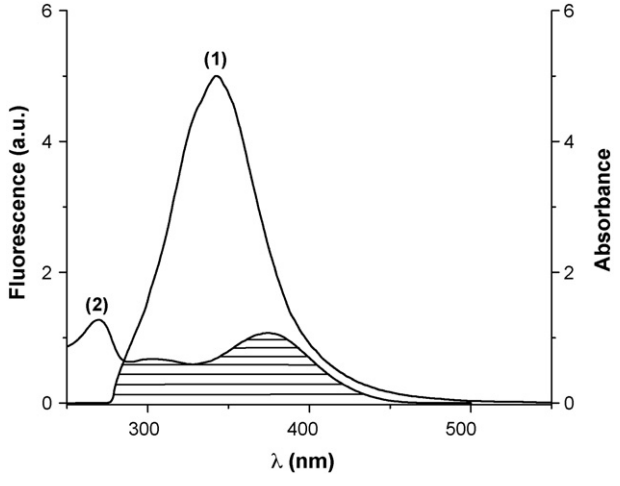

Fig. 4. Overlap of the fluorescence spectrum of HSA (1) and absorption spectrum of kaemp (2).

where E is the energy transfer efficiency, r is the D–A distance, R_0 is the critical distance ($E = 50\%$), F_0 and F are the fluorescence intensities of D in the absence and presence of an equal concentration of A [28], respectively; $k^2 = 2/3$ describes the random orientation of the D and A dipoles [8], $n = 1.333$ is the refractive index of the medium, $\Phi = 0.118$ is the fluorescence quantum yield of HSA [28] and J is the overlap integral of the emission spectrum of D and absorption spectrum of A; $F_\mathrm{D}(\lambda)$ is the corrected fluorescence intensity of D at wavelengths λ to $(\lambda + \Delta\lambda)$, with the total intensity normalized to unity, and $\varepsilon_\mathrm{A}(\lambda)$ is the molar extinction coefficient of A at wavelength λ.

The values of the Förster parameters are: $E = 0.42$, $J = 1.21 \times 10^{-14}\ \mathrm{M^{-1}\,cm^3}$, $R_0 = 2.53$ nm and $r = 2.67$ nm. An r value on the 2–8 nm scale indicates that the energy transfer occurs with high probability [29]. Furthermore, $r > R_0$ suggests the presence of a static quenching mechanism [30], in accordance with the results of steady-state fluorescence.

4. Conclusions

The binding of kaemp to HSA under physiological conditions was studied by fluorescence and circular dichroism spectroscopies. The fluorescence data indicated a strong interaction characterized by $K \sim 3.5 \times 10^5\ \mathrm{M^{-1}}$ and $n \sim 1$. The circular dichroism results evidenced partial defolding of the protein (2% loss in the α-helix), caused by a perturbation of the Trp214 residue, as ascribed by synchronous fluorescence. Hydrogen bonds are the main forces acting between kaemp and HSA. A binding distance of ~2.7 nm was computed, suggesting a high probability of the HSA–kaemp energy transfer. Our results complete the literature data available on the HSA–kaemp interaction.

Acknowledgement

We gratefully acknowledge the financial support from CNCSIS grant PN II-ID-1914 no. 494.

References

[1] E. Grotewold (Ed.), The Science of Flavonoids, vol. VIII, Springer-Verlag, Berlin, 2006.
[2] C.S. Yang, J.M. Landau, M.T. Huang, H.L. Mewmark, Annu. Rev. Nutr. 21 (2001) 381–406.
[3] E. Middelton, C. Kandaswami, T.C. Theoharides, Pharmacol. Rev. 52 (2000) 673–751.
[4] I. Hernández, L. Alegre, F. Van Breusegem, S. Munné-Bosch, Trends Plant Sci. 14 (2009) 125–132.
[5] H.M. He, D.C. Carter, Nature 358 (1992) 209–215.
[6] G. Sudlow, D.J. Birkett, D.N. Wade, Mol. Pharmacol. 12 (1975) 1052–1061.
[7] C. Dufour, O. Dangles, Biochim. Biophys. Acta 1721 (2005) 164–173.
[8] S. Bi, L. Ding, Y. Tian, D. Song, X. Zhou, X. Liu, H. Zhang, J. Mol. Struct. 703 (2004) 37–45.
[9] A. Papadopoulou, R.J. Green, R.A. Frazier, J. Agric. Food Chem. 53 (2005) 158–163.
[10] J. Tian, J. Liu, X. Tian, Z. Hu, X. Chen, J. Mol. Struct. 691 (2004) 197–202.
[11] C.D. Kanakis, P.A. Tarantilis, M.G. Polissiou, S. Diamantoglou, H.A. Tajmir-Riahi, J. Mol. Struct. 798 (2006) 69–74.
[12] B. Valeur, Molecular Fluorescence, Wiley-VCH, Weinheim, 2002, pp. 73–124.
[13] J.R. Lakowicz, Fluorescence Quenching: Theory and Applications. Principles of Fluorescence Spectroscopy, Kluwer Academic/Plenum Publishers, New York, 1999, pp. 53–127.
[14] R. Galian, A. Veglia, J. Photochem. Photobiol. A: Chem. 187 (2007) 356–362.
[15] T. Htun, J. Fluoresc. 14 (2004) 217–222.
[16] G. Xiang, C. Tong, H. Lin, J. Fluoresc. 17 (2007) 512–521.
[17] H.X. Zhang, X. Huang, P. Mei, K.H. Li, C.N. Yan, J. Fluoresc. 16 (2006) 287–294.
[18] G. Scatchard, Ann. N.Y. Acad. Sci. 51 (1949) 660–672.
[19] S. Deepa, A.K. Mishra, J. Pharm. Biomed. Anal. 38 (2005) 556–563.
[20] M. Guo, J.W. Zou, P.G. Yi, Z.C. Shang, G.X. Hu, Q.S. Yu, Analyt. Sci. 20 (2004) 465–470.
[21] Y.Z. Zhang, X. Xiang, P.M.J. Dai, L.L. Zhang, Y. Liu, Spectrochim. Acta A 72 (2009) 907–914.
[22] I.M. Klotz, Ann. N.Y. Acad. Sci. 226 (1973) 18–25.
[23] Y. Li, X. Huang, J. Xu, J. Fluoresc. 9 (1999) 173–179.
[24] F. Zsila, Z. Bikadi, M. Simonyi, Biochem. Pharmacol. 65 (2003) 447–457.

[25] H. Gao, L. Lei, J. Liu, Q. Kong, X. Chen, Z. Hu, J. Photochem. Photobiol. A: Chem. 167 (2004) 213–221.
[26] Z.X. Lu, T. Cui, Q.L. Shi, Applications of Circular Dichroism (CD) and Optical Rotatory Dispersion (ORD), Molecular Biology, Science Press, Beijing, China, 1987.
[27] T. Förster, O. Sinanoglu, Modern Quantum Chemistry, Academic Press, New York, 1966, p. 93.
[28] J.L. Yuan, I. Zhong, Z.G. Liu, Z. Hu, G. Zou, J. Photochem. Photobiol. A: Chem. 191 (2007) 104–113.
[29] Y.J. Hu, Y. Liu, L.X. Zhang, J. Mol. Struct. 750 (2005) 174–178.
[30] W.Y. He, Y. Li, C.X. Xue, Z.D. Hu, X.G. Chen, F.L. Sheng, Bioorg. Med. Chem. 13 (2005) 1837–1845.